ENGINEERING Agriculture

Engineering Journals

RESEARCH ARTICLE

2027 / Volume 14 / Issue 3 / 27734

Short-term photoaging of conventional and biodegradable mulch film microplastics: divergent surface transformation and dissolved organic matter release

Xingyu LIN*[1,2], Ying LIU*[1,3], Jing WEI[4], Lina WANG[4], Yujuan HUANG[1], Chen TU (✉)[1,3], Zheng HAO[1], Shaobai WEN[5], Xiaoping DIAO (✉)[2,6], Yongming LUO[1,3]

1 State Key Laboratory of Soil & Sustainable Agriculture, Institute of Soil Science, Chinese Academy of Sciences, Nanjing 211135, China.
2 Ministry of Education Key Laboratory for Ecology of Tropical Islands, Key Laboratory of Tropical Animal and Plant Ecology of Hainan Province, College of Life Sciences, Hainan Normal University, Haikou 571158, China.
3 College of Resources and Environment, University of Chinese Academy of Sciences, Beijing 100049, China.
4 Key Laboratory of Soil Environment Management and Pollution Control (Ministry of Ecology and Environment), Nanjing Institute of Environmental Sciences, Nanjing 210042, China.
5 The NHC Key Laboratory of Tropical Disease Control, School of Life Sciences and Medical Technology, Hainan Medical University, Haikou 571199, China.
6 State Key Laboratory of Marine Resource Utilization in South China Sea, Hainan University, Haikou 570228, China.

*These authors contribute equally to the work

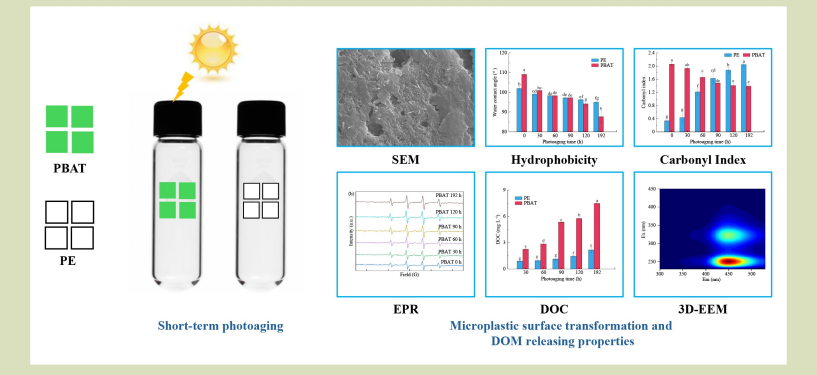
KEYWORDS

Agricultural mulch film, biodegradable microplastics, dissolved organic matter, short-term photoaging, surface transformation

HIGHLIGHTS

- Differential short-term photoaging behaviors of PE AND pbat mulch film MPs were compared.
- PBAT MPs rapidly developed porous and hydrophilic surfaces under UV irradiation.
- PE showed progressive carbonyl accumulation, whereas PBAT exhibited carbonyl loss.
- PBAT released substantially more dissolved organic matter than PE during photoaging.
- PBAT-derived DOM contained stronger humic-like signals than PE-derived DOM.

GRAPHICAL ABSTRACT



ABSTRACT

Photoaging alters microplastic (MP) surface properties and dissolved organic matter (DOM) release, yet, early-stage responses of agricultural mulch film-derived MPs remain insufficiently understood. Here, short-term (192 h) photoaging of conventional polyethylene (PE) and biodegradable poly(butylene adipate-co-terephthalate) (PBAT) MPs was investigated in

Received May 7, 2026;
Accepted June 23, 2026.

Correspondences: ctu@issas.ac.cn,
diaoxip@hainanu.edu.cn

ultrapure water under high-pressure mercury lamp irradiation in a photochemical reactor. Time-dependent changes in surface morphology, hydrophobicity, carbonyl index (CI), hydroxyl radical (·OH) formation, dissolved organic carbon (DOC), and fluorescent DOM characteristics were examined. PE and PBAT showed distinct early-stage photoaging dynamics. PBAT developed surface cracks within 30 h and became hydrophilic after 192 h, whereas PE showed obvious cracking only after 90 h and remained predominantly hydrophobic. The CI increased for PE but decreased for PBAT, indicating different surface carbonyl accumulation and loss patterns. OH signals were detected on both MPs, with stronger signals on PBAT; however, EPR results indicate radical formation rather than demonstrating the exclusive causal role of ·OH in degradation. PBAT released more DOC than PE, with DOM mainly characterized by humic- and tryptophan-like components, while PE-derived DOM was dominated by protein- and tryptophan-like substances. These findings provide an integrated solid-phase and leachate perspective on the early-stage environmental transformation of mulch-derived MPs.

© The Author(s) 2027. Published by Higher Education Press. This is an open access article under the CC BY license (http://creativecommons.org/licenses/by/4.0)

1 Introduction

Agricultural mulch films are extensively used to increase soil temperature, conserve soil moisture, suppress weeds, and improve crop yield[1,2]. In 2021, China alone consumes 1.34 million tons of agricultural mulch film per year, covering 1.78×10^7 hectares[3]. However, the limited post-use recovery and recycling of these films have led to the progressive fragmentation and accumulation of plastic residues in agricultural soils[4]. Conventional non-biodegradable plastics, particularly polyethylene (PE), have high molecular stability and may persist in the environment for decades to centuries[5,6]. Under field conditions, residual films can fragment into microplastics (MPs, < 5 mm) through solar irradiation, mechanical abrasion, tillage, and microbial activity[7,8]. The resulting MPs can alter soil physicochemical properties, impair root development, and disturb soil fauna and microbial communities[9–13].

Biodegradable plastics, especially poly(butylene adipate-co-terephthalate) (PBAT), have been promoted as alternatives to conventional PE mulch films because of their favorable mechanical properties and potential for mineralization under suitable conditions[14,15]. Nevertheless, the environmental behavior of biodegradable mulch-derived MPs remains uncertain. The ester- and carbonyl-containing structures of PBAT make it more susceptible to photochemical transformation than PE[16,17]. Previous studies have shown that photoaged biodegradable MPs may exhibit smaller particle sizes, rougher surfaces, altered wettability, and higher levels of persistent free radicals[13,18]. These processes raise concerns regarding PBAT film environmental safety, including altered interactions with coexisting pollutants and prolonged environmental persistence prior to complete mineralization[19–23].

Photoaging, involving both direct UV-induced bond cleavage and indirect radical-mediated chain scission, is a major transformation pathway for MPs in agricultural and aquatic environments[24–26]. Most existing studies on MP photoaging have focused on long-term degradation, typically over several months, particularly for widely used polymers such as PE, polypropylene (PP), and polystyrene (PS). For example, UV exposure has been shown to induce surface oxidation and microcrack formation in PE, PP, and PS under marine conditions[27]. Conversely, the short-term photoaging behavior of MPs during the initial days to weeks of exposure remains less understood, despite its importance in initiating surface oxidation, wettability changes, fragmentation, and soluble organic matter release. Recent studies have begun to explore the short-term photoaging of PBAT[28], highlighting rapid surface transformation and increased free radical formation. However, the divergent short-term photoaging dynamics of biodegradable and non-biodegradable mulch film-derived MPs remain poorly resolved, particularly with respect to the coupled evolution of solid-phase surface reactivity and aqueous dissolved organic matter (DOM) release.

To address this knowledge gap, a 192-h short-term photoaging experiment was conducted on PE and PBAT mulch film-derived microplastics in ultrapure water. The 192-h duration was selected to represent an accelerated early-stage exposure window that captures initial cracking, wettability transition, radical formation, and DOM release before extensive long-term mineralization or secondary fragmentation dominates. We tested three hypotheses: (1) PBAT undergoes earlier surface cracking and a faster transition from hydrophobicity to hydrophilicity than PE due to its photosensitive ester linkages; (2) PE and PBAT exhibit distinct carbonyl index (CI) trajectories and ·OH formation patterns, reflecting divergent oxidation and degradation pathways; and (3) PBAT releases larger amounts of DOM with different fluorescent compositions compared with PE. By characterizing surface morphology, hydrophobicity, CI, radical signals, DOC, and DOM fluorescence, this study characterizes the divergent early-stage photoaging behaviors of biodegradable and non-biodegradable mulch film-derived MPs. This work provides a cautious yet informative basis for understanding the early environmental fate of conventional and biodegradable mulch film-derived MPs in agricultural surface soils.

2 Materials and methods

2.1 Experimental materials

Black PE mulch films were obtained from Shanghai Zhentong Plastic Industry Co., Ltd., China, and black PBAT mulch films were obtained from Shandong Qingtian Plastic Industry Co., Ltd., China. Both mulch films had a uniform thickness of 0.015 mm and were manufactured in August 2023. Polymer identity was confirmed by Fourier transform infrared (FTIR) spectroscopy through comparison of the characteristic absorption bands of PE and PBAT with reference spectra. The suppliers did not disclose the detailed additive compositions or concentrations due to commercial confidentiality. However, preliminary laboratory analyses indicated the presence of plasticizers, antioxidants, and surfactants in both types of mulch films. The films were cut into 5 mm × 5 mm fragments, washed thoroughly with deionized water, and dried at 40°C for 4 h to prepare MP samples.

2.2 Photoaging experiments

For each treatment, 0.003 g of MPs and 30 mL of ultrapure water were added to 50 mL sealed quartz tubes. After ultrasonication for 30 min to ensure adequate dispersion, the tubes were placed in a photochemical reactor (XPA-VII, Xujiang Electromechanical Plant, China) equipped with a 500 W high-pressure mercury lamp at an irradiation intensity of 250 mW·cm^{-2}[29]. The reactor temperature was maintained at room temperature (20 ± 5 °C), and the suspensions were continuously stirred at 800 r·min^{-1} during irradiation. Samples were collected after 30, 60, 90, 120, and 192 h of irradiation. Ultrapure water without MPs was irradiated under identical conditions and used as a procedural blank for DOC and fluorescence analyses. In parallel, MP suspensions were incubated under identical conditions in the dark for 192 h and used as dark controls to distinguish photoaging-induced changes from non-photochemical release or transformation. All treatments were conducted in triplicate.

At each sampling time, MPs and leachates were separated using a sand-core filtration device equipped with a 0.45 μm PTFE membrane. The recovered MPs were rinsed with ultrapure water, freeze-dried for 24 h, and stored in a desiccator before further characterization. The leachates were collected in amber glass bottles and stored at 4 °C prior to DOC and fluorescence analyses.

2.3 Characterization of MP surface properties

Field-emission scanning electron microscopy (SEM, S4800, Hitachi, Japan) was used to examine the surface morphology of MPs before and after photoaging, following our previous study[30]. Water contact angles (WCA) were measured using a video contact angle analyzer (OCA20, Dataphysics, Germany) to evaluate changes in surface wettability[30]. Fourier transform infrared spectroscopy (FTIR, iS50, Thermo Fisher Scientific, USA) was used to characterize changes in MP surface functional groups[30]. The CI was calculated to quantify the degree of oxidation during photoaging. For PE, CI was calculated as the ratio of the absorbance of the carbonyl peak (C=O) at 1719 cm^{-1} to that of the methylene peak (–CH_2–) at 1462 cm^{-1}[31]. For PBAT, CI was the ratio of the carbonyl peak (C=O) at 1710 cm^{-1} to the methylene peak (–CH_2–) at 1448 cm^{-1}[28].

2.4 Reactive oxygen species (ROS) detection

Hydroxyl radicals (·OH) were detected by electron

paramagnetic resonance (EPR, EMXplus-6/1, Bruker, Germany) using 5,5-dimethyl-1-pyrroline N-oxide (DMPO) as the spin-trapping agent[32]. For each measurement, 1 mg of MPs was analyzed under the following conditions: central field, 3500 G; microwave power, 2.0 mW; scan width, 100 G; time constant, 15.0 ms; and 20 scans. Prior to EPR measurement, all samples, including non-aged controls, were irradiated under the mercury lamp for 10 min to allow sufficient accumulation of radicals on the MP surface for detection.

2.5 Leachate analysis

Dissolved organic carbon (DOC) concentrations in the leachates were quantified using a total organic carbon analyzer (TOC-L, Shimadzu, Japan). Three-dimensional excitation-emission matrix (3D-EEM) fluorescence spectra were acquired using a fluorescence spectrophotometer (F-7000, Hitachi, Japan). The emission (Em) wavelength ranged from 250 to 600 nm with a step size of 1 nm, and the excitation wavelength ranged from 200 to 450 nm with a step size of 5 nm. Parallel factor analysis (PARAFAC) was performed using MATLAB R2021a with the DOM Fluor toolbox[33,34]. The number of components was selected based on residual inspection, spectral interpretability, and comparison with the OpenFluor database[35].

2.6 Statistical analysis

Data were processed using Excel 365 and IBM SPSS Statistics 27. Differences among treatments were evaluated using one-way analysis of variance (ANOVA), followed by multiple-comparison tests when appropriate. Data are presented as mean ± standard deviation (SD, n = 3), and $p < 0.05$ was considered statistically significant. Figures were generated using Origin 2022.

3 Results and discussion

3.1 Dynamic changes in PE and PBAT MPs under short-term photoaging

3.1.1 Changes in surface morphology

Surface morphology alterations provide direct visual evidence of MP photoaging, typically reflected by increased surface roughness and the formation of cracks and pores[36,37]. Figure 1 shows the temporal evolution of surface morphology for non-biodegradable PE and biodegradable PBAT MPs during short-term UV irradiation from 0 to 192 h. Initially, PE MPs exhibited relatively smooth surfaces (Fig. 1(a)). Measurable roughness and incipient cracks were observed only after 90 h of irradiation (Fig. 1(d)). In contrast, PBAT MPs showed more pronounced surface erosion and a higher density of pores within the first 30 h of irradiation (Fig. 1(h)).

After 192 h of photoaging, PE MPs demonstrated progressive crack propagation and signs of embrittlement, although their overall structural integrity remained largely intact (Fig. 1(l)). In contrast, PBAT MPs developed larger pores and substantially rougher and more porous surfaces. The delayed crack formation observed for PE is consistent with previous findings after 108 h of photoaging[38]. The divergent morphological evolution of PE and PBAT can be attributed to their distinct polymer structures and degradation pathways. PE has high molecular stability and a large energy gap, which increases the energy barrier for electronic transition and limits chain scission during short-term photoaging. In contrast, PBAT contains photolabile ester bonds (–COO–), which can undergo cleavage to form low-molecular-weight and water-soluble products. Their subsequent leaching may contribute to pore formation and accelerated surface erosion[31].

3.1.2 Changes in hydrophilicity and hydrophobicity

WCA is widely employed to evaluate surface wettability. A WCA greater than 90° generally indicates a hydrophobic surface, whereas a value below 90° indicates a hydrophilic surface[39,40]. As shown in Fig. 2, pristine PE and PBAT MPs both showed WCA values above 90°, indicating initially hydrophobic surfaces. PBAT exhibited a significantly higher initial WCA than PE. After 60–90 h of photoaging, the WCA of PBAT gradually decreased to a level comparable to that of PE, with no significant difference between the two materials. After 120–192 h of photoaging, PBAT exhibited significantly lower WCA values than PE. Specifically, after 192 h of irradiation, the WCA of PE decreased to 95.05°, indicating that its surface remained hydrophobic. In contrast, the WCA of PBAT decreased to 87.62°, below the hydrophobicity threshold of 90°, indicating a transition from hydrophobicity to hydrophilicity. Similarly, Wang et al.[31] reported that PE remained hydrophobic after 10 d of photoaging, whereas PBAT became hydrophilic. Our results further demonstrate that a shorter exposure period of 192 h is sufficient to induce this wettability

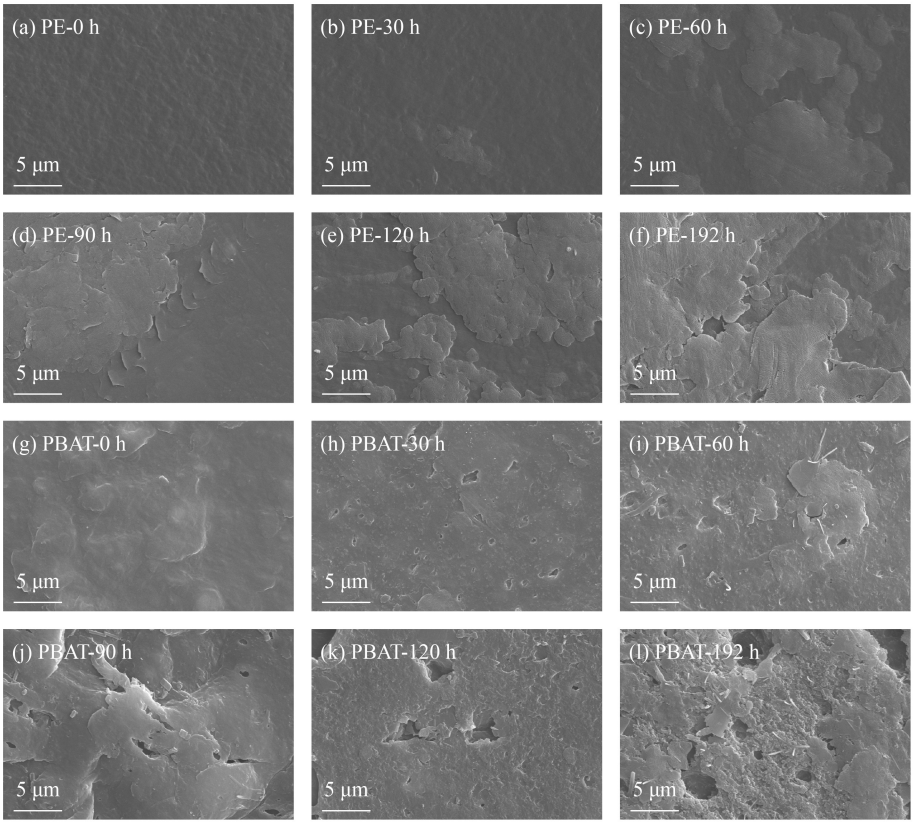


Fig. 1 Dynamic surface morphological changes of PE and PBAT MPs during 192 h of short-term photoaging. (a–f) PE MPs; (g–l) PBAT MPs.

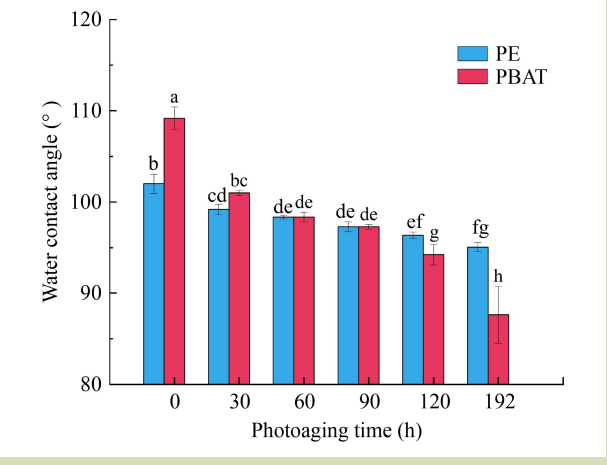


Fig. 2 Dynamic changes in the water contact angle of PE and PBAT MPs during 192 h of short-term photoaging. Data are presented as mean ± SD (n = 3). Different lowercase letters indicate significant differences among treatments at $p < 0.05$.

transition in PBAT, providing a useful temporal reference for understanding early-stage photoaging kinetics of mulch film-derived MPs.

The contrasting wettability evolution of PE and PBAT may be attributed to differences in their degradation mechanisms. PE mainly undergoes photo-oxidation during short-term aging, producing carbonyl-containing groups that may not be sufficient to induce a hydrophilic transition within 192 h[31]. Conversely, the ester bonds in PBAT are more susceptible to hydrolysis and photochemical cleavage, generating carboxyl-containing products that can further promote ester bond cleavage[41]. This process may accelerate the decrease in WCA and lead to the more rapid hydrophilic transition of PBAT. Such pronounced changes in surface wettability suggest that biodegradable MPs may undergo faster changes in interfacial behavior than conventional PE MPs. These findings indicate potential for altered adsorption-desorption interactions with coexisting pollutants[25], although direct contaminant

transport experiments are needed before ecological effects can be confirmed.

3.1.3 Changes in carbonyl index

CI is a key quantitative indicator for assessing photo-oxidative degradation of MPs, particularly the formation or loss of carbonyl-containing functional groups. As shown in Fig. 3, the CI of PE MPs increased progressively with increasing irradiation time. After 60 h of exposure, PE showed a marked increase in CI compared with pristine PE, and the CI reached its highest value of 2.04 after 192 h. A similar increasing trend in PE has been reported after 108 h of photoaging, with the CI increasing to 0.59, indicating continuous photo-oxidation[42].

Conversely, PBAT MPs showed a significant decrease in CI during the 192 h photoaging period. Notably, after 90 h, the CI value of PBAT became lower than that of PE, although the initial CI of PBAT was 2.05, approximately 6.2 times higher than that of PE at 0.33. The opposite CI trends observed for PE and PBAT suggest distinct oxidation and degradation pathways. For PE, photoaging promotes the formation of new carbonyl groups on the polymer surface, resulting in an increase in CI. However, for PBAT the decrease in CI may be associated with cleavage of ester-containing segments and the release of low-molecular-weight carbonyl-containing products, which would reduce the relative abundance of carbonyl groups

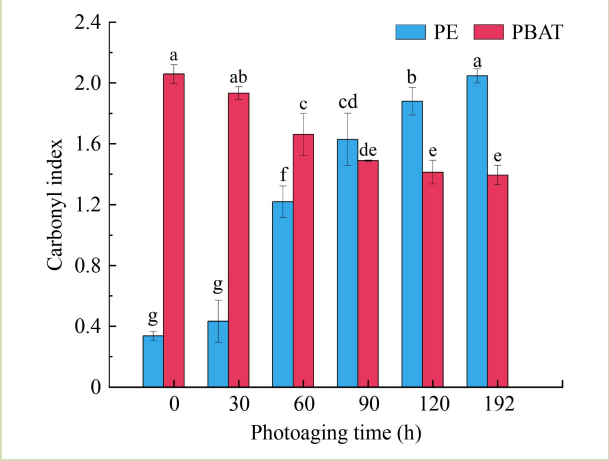


Fig. 3 Dynamic changes in the carbonyl index of PE and PBAT MPs during 192 h of short-term photoaging. Data are presented as mean ± SD (n = 3). Different lowercase letters indicate significant differences among treatments at $p < 0.05$.

remaining on the MP surface[43]. This interpretation is based on FTIR-derived CI changes and DOC/fluorescence evidence, but it is not direct proof of surface elemental changes. Further surface-sensitive analyses, such as X-ray photoelectron spectroscopy (XPS), and molecular-weight analyses, such as gel permeation chromatography, are needed to verify the chemical changes and chain scission processes underlying these divergent CI trajectories.

3.1.4 Changes in reactive oxygen species (ROS)

ROS are important participants in the photochemical degradation of MPs[44]. ROS such as ·OH, singlet oxygen ($^1O_2$) and superoxide anions ($O_2\cdot^-$) can accelerate polymer oxidation and chain scission under light irradiation[45]. Previous studies have shown that natural sunlight or simulated irradiation can induce ROS formation on MP surfaces, thereby promoting oxidative degradation[29]. As shown in Fig. 4, ·OH signals were detected on both PE and PBAT MPs throughout the 192 h photoaging period. PBAT consistently showed stronger OH signals than PE, suggesting a higher radical-generating capacity under the present accelerated irradiation conditions. This difference may be related to the structural characteristics of PBAT, including benzene rings and ester bonds (–COO–), which can facilitate electron transfer and radical formation under irradiation. Conversely, PE is composed mainly of saturated hydrocarbon chains, which limits electron transfer and leads to weaker ·OH generation[46].

The stronger OH signals on PBAT were consistent with its accelerated surface deterioration and more rapid wettability transition during short-term photoaging. Published studies indicate that during MP photoaging, polymer surface bonds can generate organic free radicals and persistent free radicals, which subsequently react with dissolved oxygen to form various ROS[28,47–49]. For PE, alkyl radicals (R·) may react with oxygen to form peroxyl radicals (ROO·), which can abstract hydrogen atoms from polymer chains and generate hydroperoxides (ROOH). Subsequent photolysis of ROOH may produce alkoxyl radicals (RO·) and ·OH, thereby promoting chain scission and the formation of oxygen-containing products[49–51]. This mechanism is consistent with the progressive increase in CI and the gradual surface deterioration observed for PE in this study. For PBAT, the aromatic terephthalate units and ester linkages may facilitate environmentally persistent free radical formation and Norrish type I/II reactions, contributing to backbone cleavage and

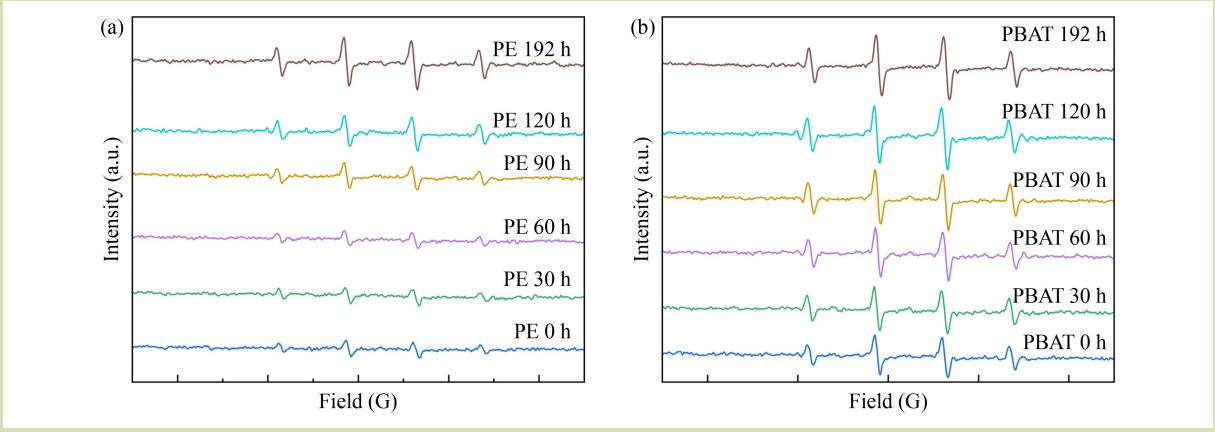


Fig. 4 Dynamic changes in ·OH signals on PE and PBAT MPs during 192 h of short-term photoaging.

oxygenated degradation products[28,31,52,53]. These literature-supported pathways provide a plausible explanation for the stronger ·OH signals, faster surface cracking, hydrophilic transition, and greater DOM release observed for PBAT compared with PE.

However, although EPR detection provides evidence of radical formation, it does not by itself establish the causal contribution of specific ROS to the observed surface transformations. Future studies should include radical quenching experiments using selective scavengers, such as isopropanol for OH, sodium azide for $^1O_2$, and benzoquinone for $O_2\cdot^-$, to clarify the relative contributions of different ROS to PE and PBAT photoaging. Such experiments would provide more direct evidence linking ROS formation and structural deterioration in PE and PBAT MPs.

3.2 Differential release of DOM from PE and PBAT MPs under short-term photoaging

3.2.1 Photoaging pathways and their influence on DOM release from MPs

In natural environments, MPs can release DOM during aging and degradation processes, and both the quantity and composition of released DOM are important indicators of polymer transformation[54,55]. As shown in Fig. 5, DOC concentrations released from both PE and PBAT MPs increased progressively with photoaging time. Throughout the 192 h irradiation period, PBAT consistently released significantly more DOC than PE, and the difference became more pronounced with prolonged irradiation. After 30 h, DOC concentrations in PBAT leachates were already significantly higher than those of PE ($p < 0.05$). After 192 h, DOC concentrations in PBAT leachate reached 7.47 mg·L^{-1}, which was more than three times higher than that of PE (2.17 mg·L^{-1}).

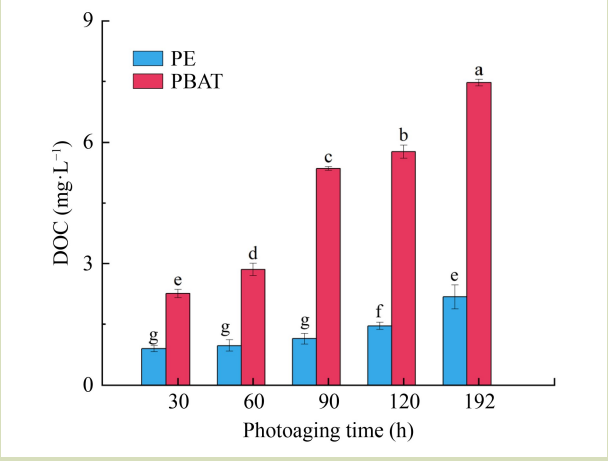


Fig. 5 Dynamic release of DOC from PE and PBAT MPs during 192 h of short-term photoaging. Data are presented as mean ± SD (n = 3). Different lowercase letters indicate significant differences among treatments at $p < 0.05$.

The substantial difference in DOC release between PE and PBAT is closely related to their distinct polymer structures and photoaging pathways. PBAT contains UV-sensitive ester

linkages and aromatic structures that are more susceptible to photolysis and radical-mediated chain scission, thereby accelerating surface cracking and pore formation (Fig. 1). These structural changes increase surface heterogeneity and may facilitate the release of low-molecular-weight organic compounds into the aqueous phase[41,56]. In addition, PBAT is a semi-crystalline polymer with relatively accessible amorphous regions that are more vulnerable to oxidative attack[57]. In contrast, PE possesses a more chemically stable hydrocarbon backbone and denser molecular structure, making it less susceptible to chain scission under equivalent irradiation conditions[53]. These observations are consistent with previous studies demonstrating polymer-dependent differences in DOM release during photoaging[38,56,58].

3.2.2 Changes in MPs-derived DOM components

Fluorescence excitation-emission matrix spectroscopy coupled with parallel factor analysis (EEM-PARAFAC) was used to characterize DOM composition associated with PE and PBAT. The PARAFAC results were interpreted using residual inspection, component interpretability, and comparison with the OpenFluor database. These compositional differences provide insight into how divergent aging pathways shape DOM molecular features, although fluorescence components should be regarded as operational fluorophore groups rather than direct molecular identification. For PE, the two fluorescent components matched protein-like and tryptophan-like spectra in OpenFluor and were therefore assigned as protein-like and tryptophan-like components.

For PE-derived DOM, fluorescence intensities increased progressively with photoaging time (Fig. 6(a–c)). This trend is consistent with slow radical-mediated oxidation of the PE hydrocarbon backbone, which can generate low-molecular-weight oxygenated fragments, including carboxylic acids, ketones, and aldehydes[59,60]. Because PE lacks hydrolysable ester bonds and has relatively high structural stability, these fluorescent products may accumulate gradually during short-term photoaging.

For PBAT-derived DOM, three fluorescent components were obtained and matched with humic-like and tryptophan-like spectra in OpenFluor; they were assigned as humic-like and tryptophan-like components (Fig. 7(a–c)). Notably, the fluorescence intensity of humic-like components decreased with photoaging time (Fig. 7(d)). This distinct compositional trajectory may arise from PBAT aging pathways involving photolysis of ester linkages and possible hydrolytic cleavage, followed by the release of soluble degradation intermediates in aqueous media[61]. The release of organic acids during PBAT photodegradation may facilitate the transformation of initial degradation products, such as aromatic fragments containing terephthalate-related structures, into smaller or weakly fluorescent molecules, consistent with observations by Ding et al.[62]. The substantially higher DOC release from PBAT compared with PE further supports more extensive polymer fragmentation, although molecular-weight analysis would be needed to directly verify chain scission.

3.2.3 Environmental implications and limitations

The observed DOC release and fluorescence changes

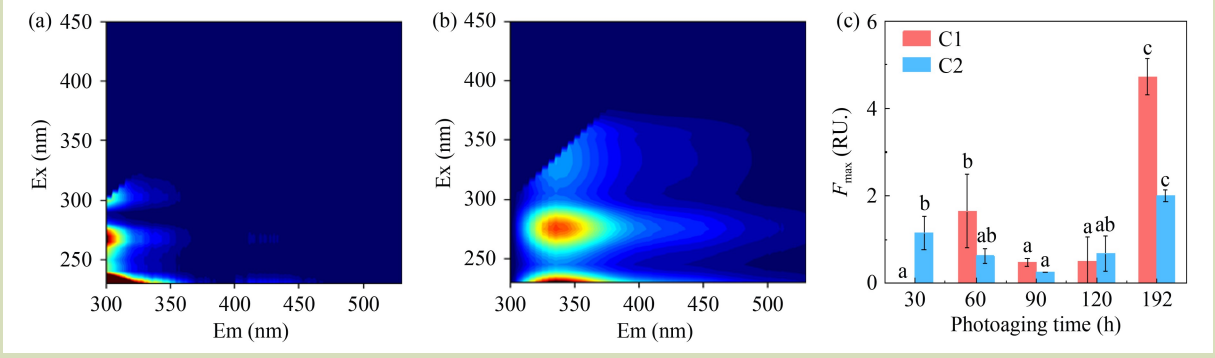


Fig. 6 Two-dimensional fluorescence patterns and changes in fluorescence intensity of PE MP leachates after different photoaging times. (a) Protein-like component (C1); (b) tryptophan-like component (C2); (c) changes in maximum fluorescence intensity (F_{max}). Data are presented as mean ± SD (n = 3). Different lowercase letters indicate significant differences among treatments at $p < 0.05$.

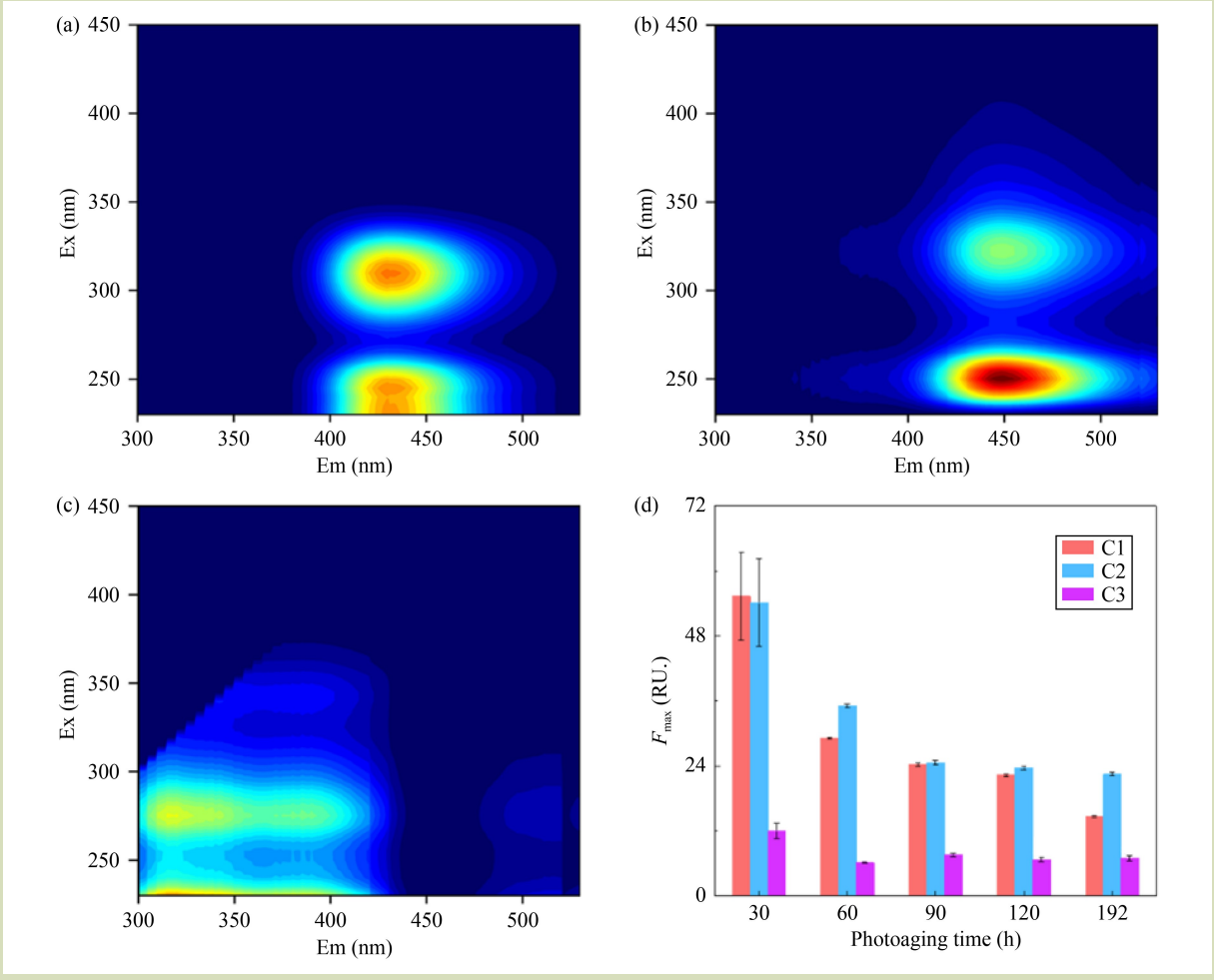


Fig. 7 Fluorescence components and changes in fluorescence intensity of PBAT MP leachates after different photoaging times. (a) Protein-like component (C1); (b) humic-like component (C2); (c) tryptophan-like component (C3); (d) changes in F_{max}. Data are presented as mean ± SD (n = 3). Different lowercase letters indicate significant differences among treatments at $p < 0.05$.

demonstrate that short-term photoaging produces polymer-specific DOM signatures. However, the present data do not directly test microbial utilization, contaminant complexation, carbon cycling, or DOM-mediated photochemical reactions. Therefore, these ecological implications should be interpreted cautiously. Additional experiments integrating microbial assays, contaminant interaction tests, photochemical reactivity measurements, and DOM optical indices would be useful for directly linking MP-derived DOM properties with environmental processes under realistic conditions.

It should also be noted that the high-pressure mercury lamp used in this study provided accelerated irradiation under controlled laboratory conditions. Its UV intensity and spectral distribution differ from those of natural sunlight and may affect the relative contributions of different photoaging pathways. Therefore, the observed transformations should be interpreted as comparative short-term reactivity patterns of PE and PBAT MPs rather than as direct predictions of field degradation rates or complete environmental degradation pathways. These findings nevertheless provide a useful basis for understanding the early transformation potential of conventional and biodegradable mulch film-derived MPs under UV exposure.

4 Conclusions

This study compared the short-term (192 h) photoaging behaviors and DOM release characteristics of PE and PBAT MPs under controlled laboratory conditions. PBAT exhibited earlier surface pore formation, a faster hydrophobic-to-hydrophilic transition, stronger ·OH signals, and greater DOC release than PE. In contrast, PE showed more limited surface alteration and remained predominantly hydrophobic after irradiation. The CI increased for PE but decreased for PBAT, indicating distinct carbonyl accumulation and loss patterns during early-stage photoaging. EEM-PARAFAC analysis further showed that PBAT-derived DOM was mainly characterized by humic-like and tryptophan-like components, whereas PE-derived DOM was dominated by protein-like and tryptophan-like components. Overall, these findings demonstrate that PBAT mulch film-derived MPs undergo faster early-stage surface transformation and DOM release than conventional PE MPs under accelerated UV irradiation. This study provides a comparative basis for understanding the early environmental transformation of conventional and biodegradable mulch film-derived MPs in agricultural surface soils.

Acknowledgements

This research was funded by the National Natural Science Foundation of China (22241602, 42177039, and 42407522), the National Key R&D Program of China (2024YFC3713900), the Major Program of State Key Laboratory of Soil and Sustainable Agriculture, China (SKLSSA2502), and the Innovative Scientific Research Project for graduates students in Hainan Province, China (Qhyb2023-160). DeepSeek-V3 was used only to assist with English language polishing. The authors reviewed and edited the final text and take full responsibility for the content.

Compliance with ethics guidelines

Xingyu Lin, Ying Liu, Jing Wei, Lina Wang, Yujuan Huang, Chen Tu, Zheng Hao, Shaobai Wen, Xiaoping Diao, and Yongming Luo declare that they have no conflicts of interest or financial conflicts to disclose. This article does not contain any studies with human or animal subjects performed by any of the authors.

REFERENCES

1. Marinari S, Mancinelli R, Brunetti P, Campiglia E. Soil quality, microbial functions and tomato yield under cover crop mulching in the Mediterranean environment. *Soil and Tillage Research*, 2015, **145**: 20–28
2. Wang J, Zhao L, Wang B Z, Mo F, Wang N, Liu S T, Song Y, Ren A T, Mei F J, Wang Y, Lu Q, Xiong Y C. Plastic film mulching ensures maize climate resilience: a perspective of temperature suitability and optimal sowing period window. *Soil and Tillage Research*, 2025, **252**: 106611
3. China National Bureau of Statistics. *China Rural Statistical Yearbook*. Beijing: *China Statistics Press*, 2024 (in Chinese)
4. Khan M A, Huang Q, Khan S, Wang Q Q, Huang J J, Fahad S, Sajjad M, Liu Y, Mašek O, Li X H, Wang J F, Song X M. Abundance, spatial distribution, and characteristics of microplastics in agricultural soils and their relationship with contributing factors. *Journal of Environmental Management*, 2023, **328**: 117006
5. Abdul Khalil H P S, Chong E W N, Owolabi F A T, Asniza M, Tye Y Y, Tajarudin H A, Paridah M T, Rizal S. Microbial-induced $CaCO_3$ filled seaweed-based film for green plasticulture application. *Journal of Cleaner Production*, 2018, **199**: 150–163
6. Sintim H Y, Bandopadhyay S, English M E, Bary A I, DeBruyn J M, Schaeffer S M, Miles C A, Reganold J P, Flury M. Impacts of biodegradable plastic mulches on soil health. *Agriculture, Ecosystems & Environment*, 2019, **273**(9): 36–49
7. Andrady A L. The plastic in microplastics: a review. *Marine Pollution Bulletin*, 2017, **119**(1): 12–22
8. Li C R, Busquets R, Campos L C. Assessment of microplastics in freshwater systems: a review. *Science of the Total Environment*, 2020, **707**: 135578
9. Enfrin M, Myszka R, Giustozzi F. Paving roads with recycled plastics: microplastic pollution or eco-friendly solution. *Journal of Hazardous Materials*, 2022, **437**: 129334
10. Gao H H, Yan C R, Liu Q, Ding W L, Chen B Q, Li Z. Effects of plastic mulching and plastic residue on agricultural production: a meta-analysis. *Science of the Total Environment*, 2019, **651**: 484–492

11. Greenfield L M, Graf M, Rengaraj S, Bargiela R, Williams G, Golyshin P N, Chadwick D R, Jones D L. Field response of N_2O emissions, microbial communities, soil biochemical processes and winter barley growth to the addition of conventional and biodegradable microplastics. *Agriculture, Ecosystems & Environment*, 2022, **336**: 108023
12. Qi Y L, Yang X M, Pelaez A M, Huerta Lwanga E, Beriot N, Gertsen H, Garbeva P, Geissen V. Macro- and micro- plastics in soil-plant system: effects of plastic mulch film residues on wheat (*Triticum aestivum*) growth. *Science of the Total Environment*, 2018, **645**: 1048–1056
13. Wang C, Gu X Y, Dong R C, Chen Z Y, Jin X, Gao J, Ok Y S, Gu C. Natural solar irradiation produces fluorescent and biodegradable nanoplastics. *Environmental Science & Technology*, 2023, **57**(16): 6626–6635
14. Serrano-Ruiz H, Martin-Closas L, Pelacho A M. Biodegradable plastic mulches: impact on the agricultural biotic environment. *Science of the Total Environment*, 2021, **750**: 141228
15. Somanathan H, Sathasivam R, Sivaram S, Mariappan Kumaresan S, Muthuraman M S, Park S U. An update on polyethylene and biodegradable plastic mulch films and their impact on the environment. *Chemosphere*, 2022, **307**(Pt 3): 135839
16. Lu J, Dong Z H, Zhou J Q, Li M, Zhang Z Z, Zhang Y, Jin R C. Biodegradable microplastics in municipal wastewater and sludge treatment processes: a review on occurrence, fate, and effects. *ACS ES&T Water*, 2024, **4**(1): 8–19
17. Zhang K, Hamidian A H, Tubić A, Zhang Y, Fang J K H, Wu C X, Lam P K S. Understanding plastic degradation and microplastic formation in the environment: a review. *Environmental Pollution*, 2021, **274**: 116554
18. Kaing V, Guo Z Y, Sok T, Kodikara D, Breider F, Yoshimura C. Photodegradation of biodegradable plastics in aquatic environments: current understanding and challenges. *Science of the Total Environment*, 2024, **911**: 168539
19. Zhu Z C, Cao X, Wang K Z, Guan Y J, Ma Y Q, Li Z Y, Guan J N. The environmental effects of microplastics and microplastic derived dissolved organic matter in aquatic environments: a review. *Science of the Total Environment*, 2024, **933**: 173163
20. Duan J J, Bolan N, Li Y, Ding S Y, Atugoda T, Vithanage M, Sarkar B, Tsang D C W, Kirkham M B. Weathering of microplastics and interaction with other coexisting constituents in terrestrial and aquatic environments. *Water Research*, 2021, **196**: 117011
21. Hu J Y, Lim F Y, Hu J Y. Characteristics and behaviors of microplastics undergoing photoaging and Advanced Oxidation Processes (AOPs) initiated aging. *Water Research*, 2023, **232**: 119628
22. Steiner T, Zhang Y H, Möller J N, Agarwal S, Löder M G J, Greiner A, Laforsch C, Freitag R. Municipal biowaste treatment plants contribute to the contamination of the environment with residues of biodegradable plastics with putative higher persistence potential. *Scientific Reports*, 2022, **12**: 9021
23. Wei X F, Bohlén M, Lindblad C, Hedenqvist M, Hakonen A. Microplastics generated from a biodegradable plastic in freshwater and seawater. *Water Research*, 2021, **198**: 117123
24. Andrady A L. Microplastics in the marine environment. *Marine Pollution Bulletin*, 2011, **62**(8): 1596–1605
25. Yu Y X, Velandia M, Hayes D G, DeVetter L W, Miles C A, Flury M. Biodegradable plastics as alternatives for polyethylene mulch films. *Advances in Agronomy*, 2024, **183**: 121–192
26. Zvekic M, Richards L C, Tong C C, Krogh E T. Characterizing photochemical ageing processes of microplastic materials using multivariate analysis of infrared spectra. *Environmental Science: Processes & Impacts*, 2022, **24**(1): 52–61
27. Gao L, Su Y Y, Mehmood T, Wang Z Z, Peng L C, Zhang N M. UVA-induced weathering of microplastics in seawater: surface property transformations and kinetics. *Frontiers in Marine Science*, 2025, **12**: 1519668
28. Wu X R, Zhang H, Chen J W, Tan F, Cai R, Wang Y. Photoaging promotes toxic micro/nanoplastics release from PLA/PBAT biodegradable plastic in gastrointestinal condition. *Environment & Health*, 2025, **3**(5): 446–457
29. Zhu K C, Jia H Z, Sun Y J, Dai Y C, Zhang C, Guo X T, Wang T C, Zhu L Y. Long-term phototransformation of microplastics under simulated sunlight irradiation in aquatic environments: roles of reactive oxygen species. *Water Research*, 2020, **173**: 115564
30. Tu C, Chen T, Zhou Q, Liu Y, Wei J, Waniek J J, Luo Y M. Biofilm formation and its influences on the properties of microplastics as affected by exposure time and depth in the seawater. *Science of the Total Environment*, 2020, **734**: 139237
31. Wang S R, Gao P, Han Q, Liu Y Q, Feng L, Zhang L Q. Insights into photoaging behaviors and mechanisms of biodegradable and conventional microplastics in soil. *Journal of Hazardous Materials*, 2024, **480**: 136418
32. Ding R, Ouyang Z Z, Bai L J, Zuo X, Xiao C Q, Guo X T. What are the drivers of tetracycline photolysis induced by polystyrene microplastic? *Chemical Engineering Journal*, 2022, **435**(Pt 1): 134827
33. Murphy K R, Stedmon C A, Graeber D, Bro R. Fluorescence spectroscopy and multi-way techniques. PARAFAC. *Analytical Methods*, 2013, **5**(23): 6557–6566
34. Wei J, Tu C, Yuan G D, Zhou Y Q, Wang H L, Lu J. Limited Cu(II) binding to biochar DOM: evidence from C K-edge NEXAFS and EEM-PARAFAC combined with two-dimensional correlation analysis. *Science of the Total Environment*, 2020, **701**: 134919
35. Murphy K R, Stedmon C A, Wenig P, Bro R. OpenFluor—An online spectral library of auto-fluorescence by organic compounds in the environment. *Analytical Methods*, 2014,

6(3): 658–661

36. Deng W B, Wang Y J, Wang Z H, Liu J X, Wang J, Liu W J. Effects of photoaging on structure and characteristics of biofilms on microplastic in soil: biomass and microbial community. *Journal of Hazardous Materials*, 2024, **467**: 133726
37. He J H, Ma W W, Han L F, Chen L Y, Xu E G, Xing B S, Yang Z F. Unraveling the role of natural and pyrogenic dissolved organic matter in photodegradation of biodegradable microplastics in freshwater. *Carbon Research*, 2023, **2**: 18
38. Wang H Q, Zhu J H, He Y, Wang J W, Zeng N D, Zhan X H. Photoaging process and mechanism of four commonly commercial microplastics. *Journal of Hazardous Materials*, 2023, **451**: 131151
39. He Y, Xiao S P, Wu J J, Fang H. Influence of multiple factors on the wettability and surface free energy of leaf surface. *Applied Sciences*, 2019, **9**(3): 593
40. Wang J C, Yue D B, Wang H. *In situ* Fe_3O_4 nanoparticles coating of polymers for separating hazardous PVC from microplastic mixtures. *Chemical Engineering Journal*, 2021, **407**: 127170
41. Liu T Y, Zhen Z C, Zang X L, Xu P Y, Wang G X, Lu B, Li F, Wang P L, Huang D, Ji J H. Fluorescence tracing the degradation process of biodegradable PBAT: visualization and high sensitivity. *Journal of Hazardous Materials*, 2023, **454**: 131572
42. Wang L L, Guo C X, Qian Q Q, Lang D N, Wu R L, Abliz S, Wang W, Wang J D. Adsorption behavior of UV aged microplastics on the heavy metals Pb(II) and Cu(II) in aqueous solutions. *Chemosphere*, 2023, **313**: 137439
43. Meng X Z, Ye Y, Yang R. Computational and experimental study on the mechanism of CO_2 production during photo-oxidative degradation of poly(butylene adipate-*co*-terephthalate): differences between PBA and PBT segments. *Macromolecules*, 2023, **56**(19): 7749–7762
44. Qiu X R, Ma S R, Zhang J X, Fang L C, Guo X T, Zhu L Y. Dissolved organic matter promotes the aging process of polystyrene microplastics under dark and ultraviolet light conditions: the crucial role of reactive oxygen species. *Environmental Science & Technology*, 2022, **56**(14): 10149–10160
45. Li Q Y, Cao J C, Li J, Li D D, Jing B H, Zhou J H, Ao Z M. Novel insights into photoaging mechanisms and environmental persistence risks of polylactic acid (PLA) microplastics: direct and indirect photolysis. *Science of the Total Environment*, 2024, **954**: 176350
46. Qiu X R, Wang X X, Pan J R, Ding L, Liang X J, Guo X T. Significant contribution of different sources of particulate organic matter to the photoaging of microplastics. *Water Research*, 2024, **251**: 121173
47. Wang J, Liu S T, Chen S N, Long Y X, Lou Y, Ren N Q, Ma J, Xing D F. Insights into the photoaging behavior of microplastics: environmental fate and ecological risk. *Environmental Science & Technology*, 2025, **59**(44): 23673–23690
48. Duan J J, Li Y, Gao J N, Cao R Z, Shang E X, Zhang W. ROS-mediated photoaging pathways of nano- and micro-plastic particles under UV irradiation. *Water Research*, 2022, **216**: 118320
49. Tang Y, Fan K Q, Herath I, Gustave W, Lin C X, Qin J H, Qiu R L. Contribution of free hydroxyl radical to the formation of micro(nano)plastics and release of additives during polyethylene degradation in water. *Environmental Pollution*, 2023, **337**: 122590
50. Meng X Z, Jin G X, Yang R. A quantum chemical and molecular dynamics simulation study on photo-oxidative aging of polyethylene: mechanism and differences between crystalline and amorphous phases. *Polymer Degradation and Stability*, 2023, **217**: 110536
51. Maurer-Jones M A, Monzo E M. Quantifying photochemical transformations of poly(butylene adipate-*co*-terephthalate) films. *ACS Applied Polymer Materials*, 2021, **3**(2): 1003–1011
52. Chen X, Yue Y Y, Wang Z H, Sun J H, Dong S Y. Co-existing inorganic anions influenced the Norrish I and Norrish II type photoaging mechanism of biodegradable microplastics. *Science of the Total Environment*, 2024, **925**: 171756
53. Yang Y, Li Z, Yan C R, Chadwick D, Jones D L, Liu E K, Liu Q, Bai R H, He W Q. Kinetics of microplastic generation from different types of mulch films in agricultural soil. *Science of the Total Environment*, 2022, **814**: 152572
54. Zhang J, Hou X F, Zhang K N, Deng Y W, Xiao Q Z, Gao Y, Zhou X X, Yan B. Deciphering fluorescent and molecular fingerprint of dissolved organic matter leached from microplastics in water. *Water Research*, 2024, **250**: 121047
55. Ouyang Z Z, Li S X, Xue J C, Liao J M, Xiao C Q, Zhang H, Li X H, Liu P, Hu S W, Guo X T, Zhu L Y. Dissolved organic matter derived from biodegradable microplastic promotes photo-aging of coexisting microplastics and alters microbial metabolism. *Journal of Hazardous Materials*, 2023, **445**: 130564
56. Li X J, Tan D Y, Xie L, Sun H J, Sun S Y, Zhong G J, Ren P G. Effect of surface property of halloysite on the crystallization behavior of PBAT. *Applied Clay Science*, 2018, **157**: 218–226
57. Wang Z G, Ding J N, Song X J, Zheng L X, Huang J C, Zou H, Wang Z Y. Aging of poly (lactic acid)/poly (butylene adipate-*co*-terephthalate) blends under different conditions: environmental concerns on biodegradable plastic. *Science of the Total Environment*, 2023, **855**: 158921
58. Wang K, Xu S J, Wang J Z, Gao B Q, Huang Y, Song J, Ma S L, Jia H Z, Zhan S H. Insights into the photosensitivity and photobleaching of dissolved organic matter from microplastics: structure-activity relationship and transformation mechanism. *Journal of Hazardous Materials*, 2024, **480**: 135931
59. Peacock A J. The chemistry of polyethylene. *Journal of*

Macromolecular Science, Part C: Polymer Reviews, 2001, **41**(4): 285–323

60. Gardette J L, Therias S. Photooxidation of polyethylene: chemical mechanisms and advanced characterization strategies. *Journal of Vinyl and Additive Technology*, 2026, **32**(4): 854–864
61. Zhou Q, Pan C N, Wei J A, Ma Z Y, Liu B S, Zhang D Y, Wei J, Pan X L. Biodegradable plastics in soil: a significant gap from microplastics to nanoplastics and oligomers. *Environmental Science: Nano*, 2025, **12**(4): 2208–2228
62. Ding L, Zhang H W, Chen H, Zhang G D, Qiu X R, Zhang B, Liang X J, Wei J, Guo X T. Photochemical transformation of microplastics-derived dissolved organic matter altered the photoaging of microplastics. *Journal of Hazardous Materials*, 2025, **500**: 140477